Received: 15 April 2020 | Revised: 11 July 2020 | Accepted: 13 July 2020

DOI: 10.1002/bip.23394



FULL PAPER

Biopolymers WILEY

# RNA-based fluorescent biosensors for live cell detection of bacterial sRNA

Rebekah Z. Kitto[1,2] | Kylee E. Christiansen[2] | Ming C. Hammond[1,2]

[1]Department of Chemistry, University of California, Berkeley, California, USA

[2]Department of Chemistry and Henry Eyring Center for Cell and Genome Sciences, University of Utah, Salt Lake City, Utah, USA

**Correspondence**
Ming C. Hammond, Department of Chemistry, University of Utah, Salt Lake City, Utah.
Email: mingch@chem.utah.edu

**Funding information**
Division of Molecular and Cellular Biosciences, Grant/Award Number: 1815508; National Institute of General Medical Sciences, Grant/Award Numbers: R01GM124589, T32GM122740

## Abstract

Bacteria contain a diverse set of RNAs to provide tight regulation of gene expression in response to environmental stimuli. Bacterial small RNAs (sRNAs) work in conjunction with protein cofactors to bind complementary mRNA sequences in the cell, leading to up- or downregulation of protein synthesis. *In vivo* imaging of sRNAs can aid in understanding their spatiotemporal dynamics in real time, which inspires new ways to manipulate these systems for a variety of applications including synthetic biology and therapeutics. Current methods for sRNA imaging are quite limited *in vivo* and do not provide real-time information about fluctuations in sRNA levels. Herein, we describe our efforts toward the development of an RNA-based fluorescent biosensor for bacterial sRNA both *in vitro* and *in vivo*. We validated these sensors for three different bacterial sRNAs in *Escherichia coli* and demonstrated that the designs provide a bright, sequence-specific signal output in response to exogenous and endogenous RNA targets.

**KEYWORDS**

biosensor, flow cytometry, sRNA

## 1 | INTRODUCTION

Bacterial sRNAs are regulatory RNAs that alter gene expression patterns in response to changes in the cellular environment.[1,2] Certain sRNAs are essential to metabolic processes, and levels fluctuate in the presence or absence of potential nutrients.[3] However, some sRNAs are only expressed during specific stages of infection, allowing pathogens to produce the proteins necessary for host cell invasion.[4] In addition to numerous native functions in bacteria, sRNAs have also been adapted for synthetic biology applications. Partially modified and/or completely artificial sRNA constructs have been developed for the external regulation of both exogenous and endogenous genes. These engineered sRNAs have been successfully employed to improve bacterial synthesis of target compounds, including fuel precursors[5] and food additives.[6]

Traditionally, cellular sRNA levels can be measured through RT-PCR[7] and Northern blotting, both requiring lysis of the bacteria of interest.[8,9] Therefore, these methods do not provide real-time detection of sRNA levels in live cells. Recent work has shown that genetically encodable, RNA-based sensors can be used for sRNA detection and sub-cellular localization *in vivo*.[10,11] These designs provide a specific, amplified response to a target sRNA that can be monitored in live cells. However, these methods rely on a catalytic assembly or signal cascade event to accumulate fluorescent signal gradually over time, so function more as reporters than real-time sensors. As a result, another sensor design strategy is necessary to visualize and quantify fluctuations in sRNA levels in response to changes in surrounding environments. An RNA-based fluorescent biosensor would provide the same advantage of genetic encodability while being able to respond to real-time changes in engineered and native sRNAs within the cell.

Previously, our group has shown that riboswitches can be successfully adapted to develop RNA-based fluorescent (RBF) biosensors for small molecule signals and metabolites in bacteria.[12–18] In addition, other groups have developed RBF biosensors for miRNA and mRNA detection in eukaryotes.[19–23] Unlike riboswitch-based designs for small-molecule sensing, these sensors: (a) directly hybridize to their target RNA sequence, and (b) are artificially designed through rational engineering or computational processes. Most of these RNA-sensing systems were shown to function in eukaryotes, but only

  

recently have bacterial applications been explored.[22,23] In addition, the FASTmiR (Fluorescent Aptamer Sensor for Tracking miRNA) system designed for miRNA detection has not yet been adapted for the detection of larger RNA targets, such as sRNAs or mRNAs.

In this study, we present the in silico design of RBF biosensors that can detect the bacterial sRNAs RyhB, SgrS, and PinT. RyhB and SgrS are native to *E coli* and are involved in iron and sugar metabolism, respectively. PinT is found in *Salmonella enterica* and is known to be directly involved in virulence and infection processes. These sensors were computationally designed through customization of a previously published miRNA sensor sequence from the FASTmiR system.[20] The function of two circular permutations of the Spinach aptamer, modSpinach, and cpSpinach2, were compared in these sensors. Candidate designs were screened *in vitro* to produce several successful designs for each sRNA target. These hits were then evaluated in live *E coli* and were able to detect both exogenous and endogenous sRNAs.

## 2 | MATERIALS AND METHODS

### 2.1 | ViennaRNA modeling

RNA modeling was performed using ViennaRNA fold and cofold software packages.[24] Twenty-one nucleotide fragments of the sRNA target were generated using a Python script and checked on NCBI BLAST (National Center for Biotechnology Information Basic Local Alignment Search Tool)[25] to ensure that they would not have off-target complementarity in the *E coli* (or *S enterica*, for PinT) genome. Sequences were then ported into Aquamacs software and manually checked for desired folding criteria with and without target. For mock sRNA testing, overhangs from the original FASTmiR design[20] were kept in place and criteria were met. FASTsRNA sequences did not display proper folding with original overhangs, so manually inserted overhangs were used to obtain the desired folding patterns. Overhang-induced folding changes were difficult to predict and required testing

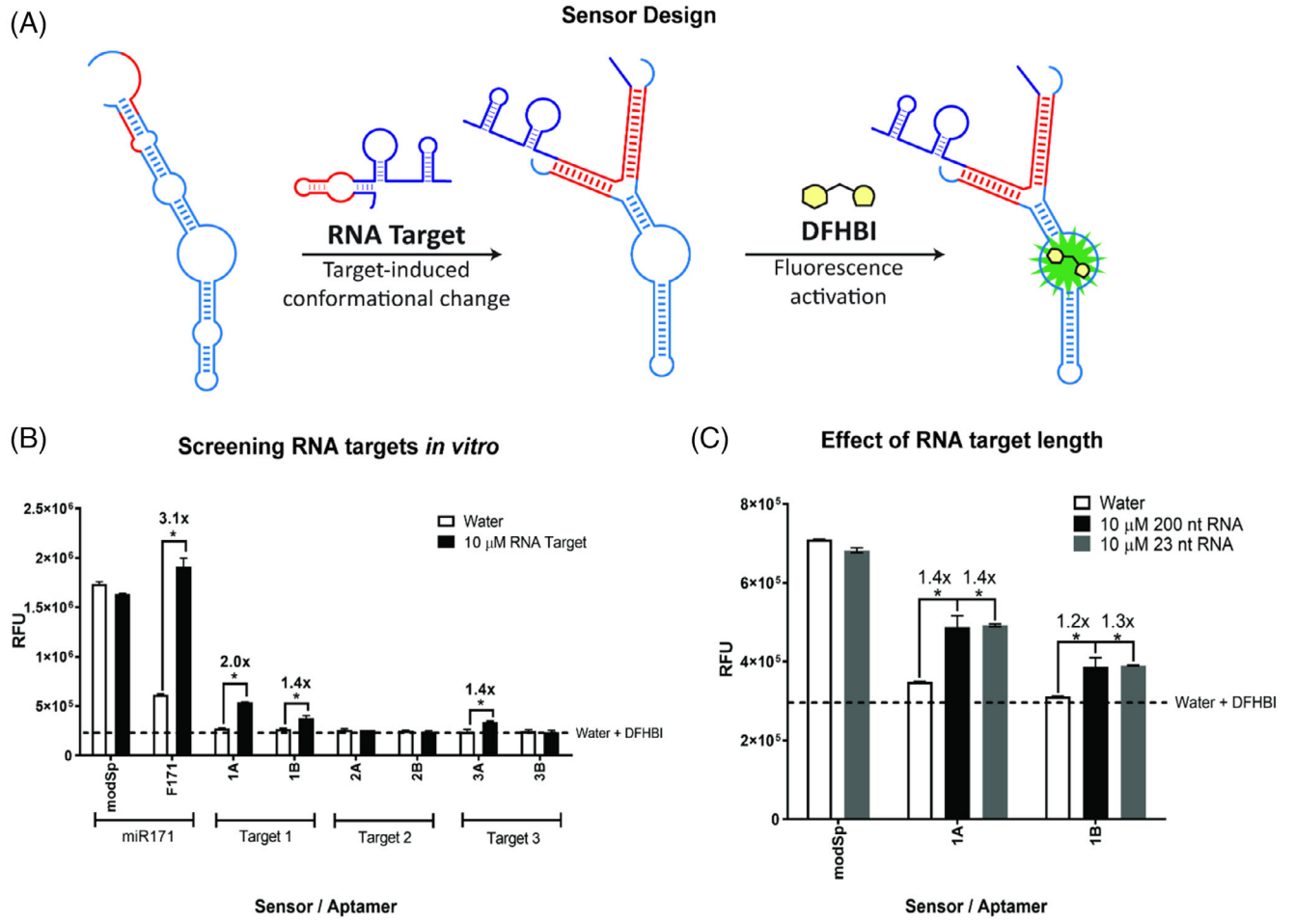


**FIGURE 1** FASTsRNA mechanism and initial testing. A, Schematic illustrating a representative FASTsRNA sensor, based on the FASTmiR design method. In the off configuration, the sensor contains an unstructured G-quadruplex within the Spinach-based aptamer sequence (modSpinach or cpSpinach2). The sensory domains hybridize to a 21-23 nt sequence within a target sRNA through toehold-mediated displacement, reconstituting the G-quadruplex in the Spinach-based aptamer and allowing DFHBI to bind, producing a fluorescent output. B, Performance of FASTsRNA in 10 mM Tris–HCl, pH 7.5, 100 mM NaCl, 1 mM $MgCl_2$ with 5 μM sensor and 10 μM target RNA at 37 °C. Three different 200-nt mock sRNA targets were used to test six FASTsRNA designs, with a total of three hits showing a statistically significant response to the target sequence (*P*-value < .05 are starred). C, Interrogation of the effects of target RNA length on FASTsRNA sensor activity

of 20 to 25 sensor sequences with >10 overhangs for each target. Final hits were taken forward for molecular cloning.

## 2.2 | Molecular cloning

Oligonucleotides for FASTsRNA cloning were ordered from the University of Utah Core Laboratories and IDT (Integrated DNA Technologies). Complementary oligonucleotides were used to create cpSpinach2 and modSpinach backbones onto which 5′ and 3′ sensory domains were added via overlap extension PCR.[26] DFHBI and DFHBI-1T were synthesized as previously described[27,28] or ordered from Tocris Biosciences.

FASTsRNA sequences were constructed using overlap extension PCR to add sensory domains onto modSpinach or cpSpinach2 backbone sequences. Sequences for all target RNA and sensors can be found in Tables S1 and S2, respectively. Complete primer list for each sensor is given in Table S3. For *in vitro* testing, sequences were PCR-amplified to include the T7 promoter and produced through run-off transcription.

For *in vivo* testing, FASTsRNA sensors were cloned into a pRSET-B vector (Thermo Fisher Scientific) and full-length bacterial sRNA targets were cloned into the pET24a(+) plasmid. Cloning inserts were first constructed via overlap-extension PCR[26] and inserted into their respective plasmids using Gibson assembly.[29] Both sensor and target RNAs were designed to be expressed under an IPTG-inducible T7 promoter sequence and terminated with a terminator sequence. For the Gibson assembly, the pRSET-B vector was PCR amplified to give the linear form. The linear vector of the pET24a(+) plasmid was also obtained by restriction digest with BglII and XhoI. Following linearization of the target plasmids, both vector and insert were added to a previously prepared Gibson master mix containing T5 exonuclease, Phusion polymerase, Taq DNA ligase, and ISO reaction buffer. After incubation at 20 °C for 1 hour, the mixture was immediately transformed into Top10 cells (MacroLab) through standard heat shock protocol, plated on LB agar with appropriate antibiotic, and incubated overnight at 37 °C. Construct sequences

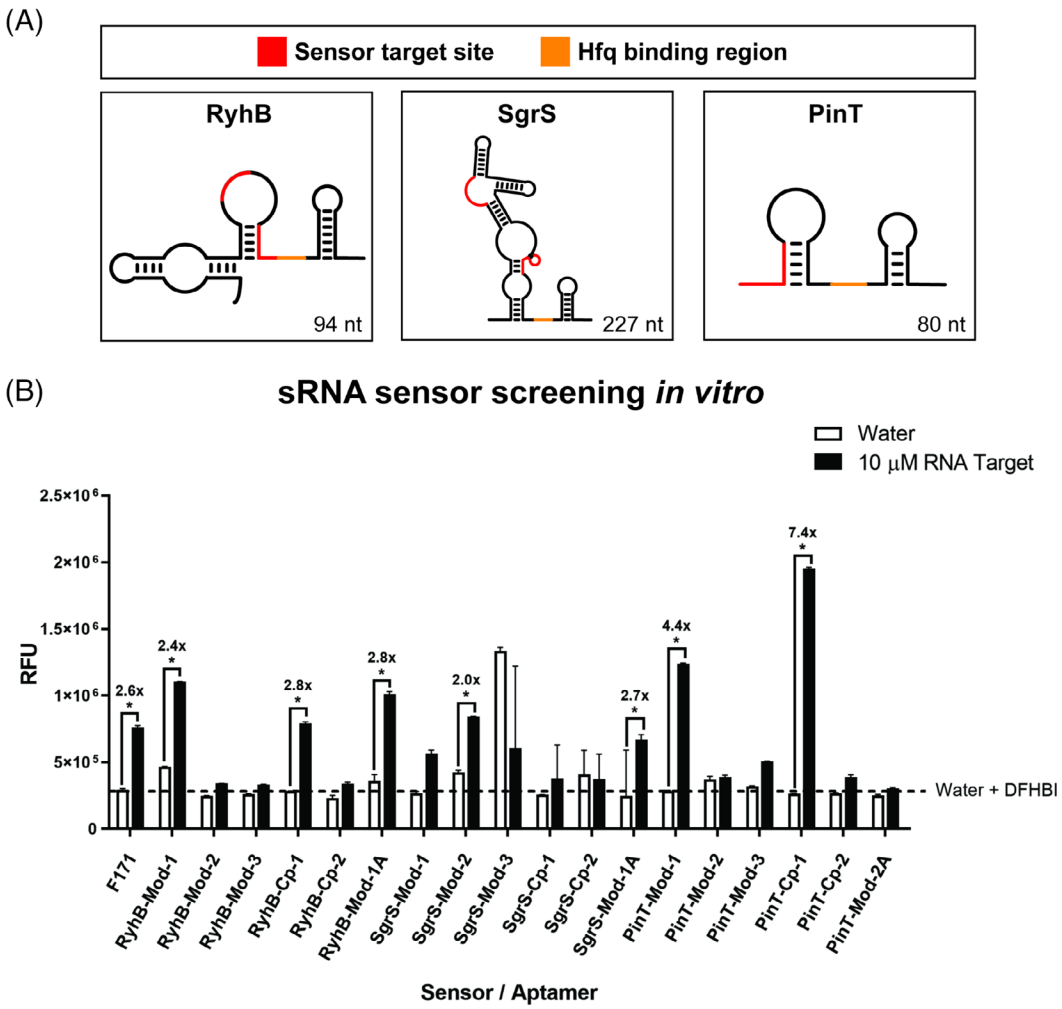


**FIGURE 2** FASTsRNA design and validation. A, Predicted secondary structure for the three target sRNA sequences. The sensor hybridization regions are highlighted in red and the predicted Hfq binding site is shown in orange. B, Screening of selected sensor candidates after ViennaRNA folding predictions. A total of eight sensors produced a fluorescent response to the sRNA sequences, and two hits were chosen for each target. Dashed line represents the average water-DFHBI background signal level

were confirmed by sequencing plasmids (University of Utah Sequencing Core Facility). For *in vivo* experiments, sensor and sRNA plasmids were constructed using the cloning procedure described above and subsequently transformed into *E coli* BL21 (DE3) Star cells (MacroLab).

### 2.3 | *In vitro* fluorescence assays

All sensors were prepared as previously described.[13,30] Briefly, templates were amplified from plasmid sequences to contain T7 promoter + sensor. Transcription was then performed with T7 RNA polymerase and the products were purified using either a denaturing 6% Urea-PAGE gel or the Zymo RNA Clean and Concentrator kit, depending on product purity after transcription. Following purification, the RNA was quantified through thermal hydrolysis.[31]

Fluorescence assays for the FASTsRNA experiments were performed as previously described,[13] but under modified buffer and refolding conditions. Each well contained sensor RNA, target RNA, and DFHBI in a binding buffer (10 mM Tris-HCl, 100 mM NaCl, 1 mM $MgCl_2$, pH 7.5 with 5-10 μM sensor, and 5-10 μM target RNA). Both sensor and target RNAs were independently refolded in buffer by heating to 95 °C for 10 minutes, then slowly cooling to room temperature before setting up the assay. Other assay components were added to each well, then, the sensor and target RNAs were added just before analysis. The reaction plate was preincubated at the read temperature the fluorescence was measured using the i3X plate reader (Molecular Devices) at 448 nm excitation and 506 nm emission. Reads were taken every 5 minutes over a 1 hour period and the final data analysis was performed on measurements after sensor equilibration.

### 2.4 | Flow cytometry analysis of *in vivo* fluorescence

Flow cytometry experiments were conducted as previously described.[14] Cultures containing co-expressed sensor and target plasmids were grown overnight in ZYP-5052 autoinduction media for 16 hours.[32] Cells were then diluted 1:50 into 1X PBS, pH 7.4 with 100 to 500 μM DFHBI-1T and added to a plate. Samples were then measured on an Attune NxT (Thermo Fisher) flow cytometer capturing at least 30 000 events with a 488 nm laser and 530 nm filter. Mean fluorescence intensity for each population was quantified and graphed using FlowJo software.

## 3 | RESULTS AND DISCUSSION

### 3.1 | FASTsRNA performance *in vitro*

The previously published FASTmiR design incorporates a modified Spinach (modSpinach) aptamer core sequence that binds to DFHBI, an analog of the green fluorescent protein chromophore, and terminal sensory domains that hybridize to a 21-nucleotide (21 nt) target RNA. In the sensor's "OFF" configuration, the aptamer is misfolded, and the terminal regions contain a toehold-mediated displacement sequence that can bind to a target. The sensor undergoes a conformational change upon hybridizing to the target sRNA, which should reconstitute the binding pocket for the fluorescent dye ligand (Figure 1A).

While miRNAs are typically 21 to 25 nt in length, sRNAs can contain up to 500 nt. Therefore, to initially determine whether the FASTmiR sensor design would be useful for detecting bacterial RNA with longer sequences, six preliminary sensors (two per target RNA) were designed to target three arbitrary 200 nt RNA sequences. The 21 nt region of hybridization within each target RNA was selected

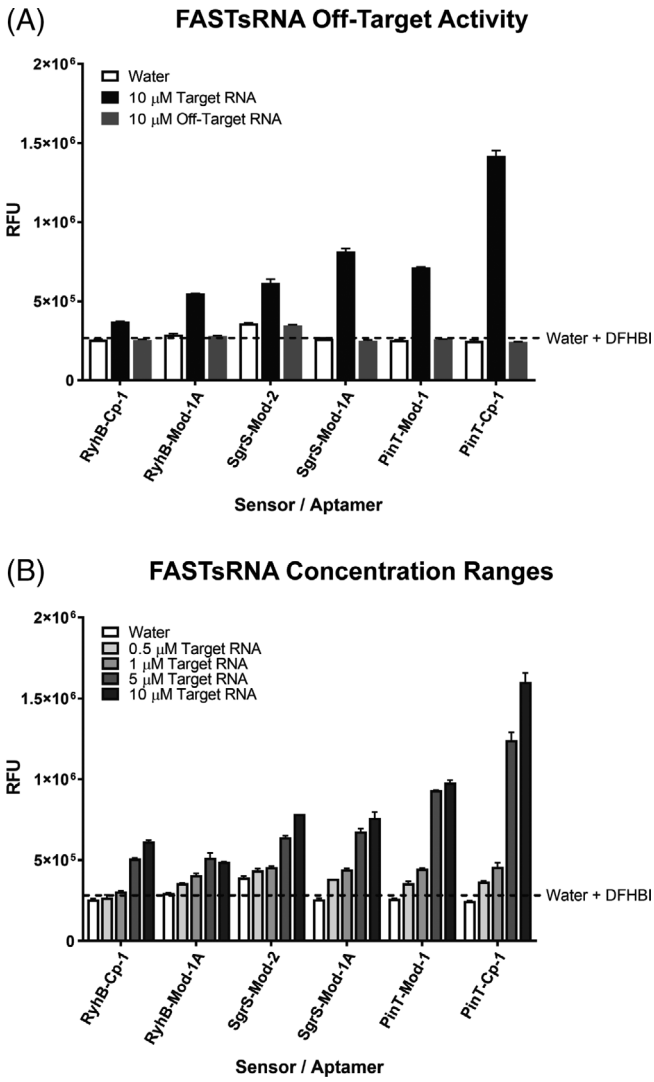


**FIGURE 3** FASTsRNA characterization. Fluorescence plate reader data for FASTsRNA sensors testing off-target activity and response to different target sRNA concentrations. Screen performed in buffer (10 mM Tris–HCl, pH 7.5, 100 mM NaCl, 1 mM $MgCl_2$) with 5 μM sensor and 5-10 μM target RNA at 37 °C. Dashed line represents water-DFHBI background signal. A, FASTsRNA designs tested against on- and off-target sRNA for turn-on. PinT sensors were tested with RyhB, RyhB sensors with SgrS, and SgrS sensors with PinT for off-target screen. B, Sensors were incubated with 5, 10, and 15 μM target sRNA to determine approximate working range

using the ViennaRNA cofold software to evaluate three criteria for the predicted RNA structures: (a) Disruption of the fluorescent aptamer G-quadruplex in the unbound "OFF" configuration, (b) Presence of toehold binding regions complementary to the target RNA, and (c) Energetically favorable transition to the bound "ON" configuration (Figure S1). Sensors that met all three criteria were taken forward for validation with target RNAs *in vitro* and were tested alongside a representative FASTmiR sensor (F171) and its target miRNA (miR171) to compare sensor activity. Each sensor and target RNA were synthesized by *in vitro* transcription using T7 RNA polymerase followed by PAGE purification. The FASTmiR sensor exhibited a 3.1-fold turn-on, while sensors 1A, 1B, and 3A also showed statistically significant turn-on with fold activations between 1.4x and 2.0x when exposed to their respective target RNAs in binding buffer (10 mM Tris-HCl, 100 mM NaCl, 1 mM $MgCl_2$, pH 7.5). In contrast, the Spinach control showed no response to RNA (Figure 1B). Additionally, the sensors suffered no loss of performance between short 23 nt targets and longer 200 nt sequences with embedded target regions, as seen by the nearly identical fold activation (Figure 1C). These data indicate that the FASTmiR method is amenable to longer RNA targets.

Moving forward, several more sensors we called FASTsRNA sensors were designed using the same criteria above to target specific regions of three different sRNAs: RyhB (94 nt) and SgrS (227 nt) from *E coli*, and PinT (80 nt) from *S enterica*. In an effort to improve fluorescence signal, the original core modSpinach aptamer of some sensor designs was replaced with a circularly permuted version of Spinach2 (cpSpinach2), as Spinach2 is an optimized version of the Spinach aptamer.[33] Additionally, cpSpinach2 has exhibited robust fluorescent signal in bacteria with a single sensor copy,[34] while modSpinach required multiple copies to function optimally.[20] A total of five predicted functional sensors were computationally designed for each sRNA target, with three containing modSpinach and two containing cpSpinach2. An additional modSpinach design was also included as a predicted negative control, having failed to meet one or more of the aforementioned design criteria (Figure S1).

Each sensor was named according to their target sequence, which dye-binding aptamer is present (modSpinach or cpSpinach2), and a number corresponding to different hybridization regions within the target RNA. Control sequences end with an A and have the same sensory regions as the sensor designated by the first three identifiers (SgrS-Mod-1A binds the same target region as SgrS-Mod-1). To prevent off-target binding, all sensory domains were designed to contain no more than 5 nt complementarity to other native RNAs in the cell. Furthermore, to minimize interference with native sRNA function inside cells, the target regions were selected to be outside of the

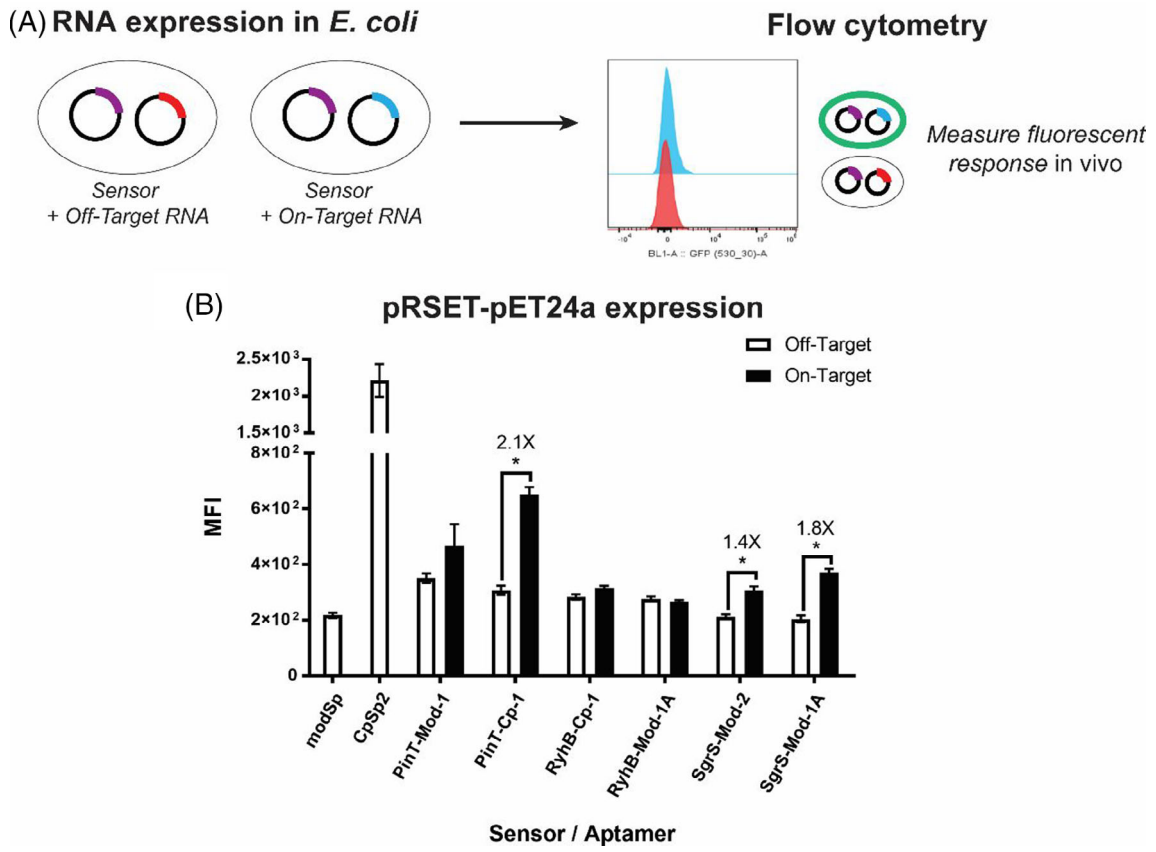


**FIGURE 4** FASTsRNA sensor performance *in vivo*. Flow cytometry data for FASTsRNA sensors. A, Workflow for sensor testing in *E coli*. Dual plasmid expression under the T7 promoter was used to compare sensor + on-target sRNA and sensor + off-target sRNA. B, MFI (mean fluorescence intensity) was calculated through flow cytometry analysis and plotted for each FASTsRNA sensor

predicted AU-rich binding region for the chaperone protein, Hfq, which is necessary for proper function of many sRNAs in both *E coli* and *S enterica* (Figure 2A).[35–39]

Sensor candidates were screened *in vitro* in the presence of their respective full-length RNA targets. RyhB-Mod-1, RyhB-Cp-1, RyhB-Mod-1A, SgrS-Mod-2, and SgrS-Mod-1A all showed statistically significant fluorescent response similar to the FASTmiR sensor (between 2.0 and 2.7-fold turn-on) with 10 μM sRNA target, while PinT-Mod-1 and PinT-Cp-1 exhibited a fold activation greater than that of the FASTmiR sensor (Figure 2B). One cpSpinach2-based design, PinT-Cp-1, displayed the greatest fluorescence activation at >7-fold. Interestingly, both PinT-Cp-1 and PinT-Mod-1 were designed to bind the same target sequence of the PinT sRNA, but they contained the cpSpinach2 and modSpinach aptamers, respectively. The modSpinach design showed only a four-fold turn-on in this initial screen, indicating that cpSpinach2 does indeed outperform modSpinach. No other clear trends were observed after inspecting the ViennaRNA parameters for each of the active designs (Figure S2). In fact, several of the predicted negative controls (RyhB-Mod-1A and SgrS-Mod-1A) showed a significant response to their target sRNA sequences. As a result, we suspect that the ViennaRNA predictions have limited application for accurate prediction of sensor designs, which has also been seen for artificial riboswitch designs.[40] This modeling method led to a good candidate hit rate (~33%) but there is a possibility of dismissing successful designs that were predicted to be misfolders, and vice versa.

The top two hits for each target RNA were further characterized *in vitro*. To probe the specificity of each sensor for their target, the sensors were tested against one of the other sRNA targets to simulate off-target binding interaction (e.g., RyhB sensors were tested with SgrS RNA as off-target). All designs showed a clear fluorescent signal when tested with the appropriate sRNA but no activation in the presence of off-target RNA (Figure 3A). Each sensor was responsive for target RNA concentrations between 0.5 and 10 μM. However, PinT-Cp-1, RyhB-Cp-1, SgrS-Mod-2, and SgrS-Mod-1A exhibited a dose-dependent response over this concentration range, whereas PinT-Mod-1 and RyhB-Mod-1A appeared to be saturated at 10 μM of target (Figure 3B), suggesting a higher affinity of the latter sensors for their target RNA. These results indicate that the sensors may be selective and sensitive enough to detect native sRNAs in bacteria.

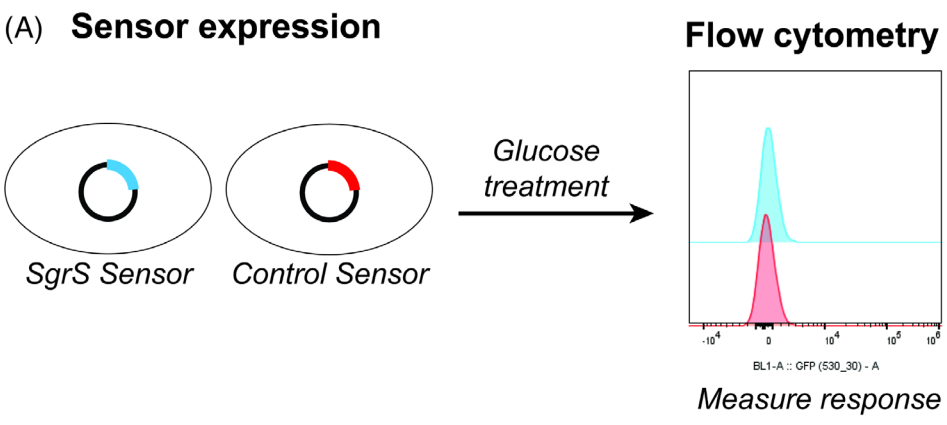


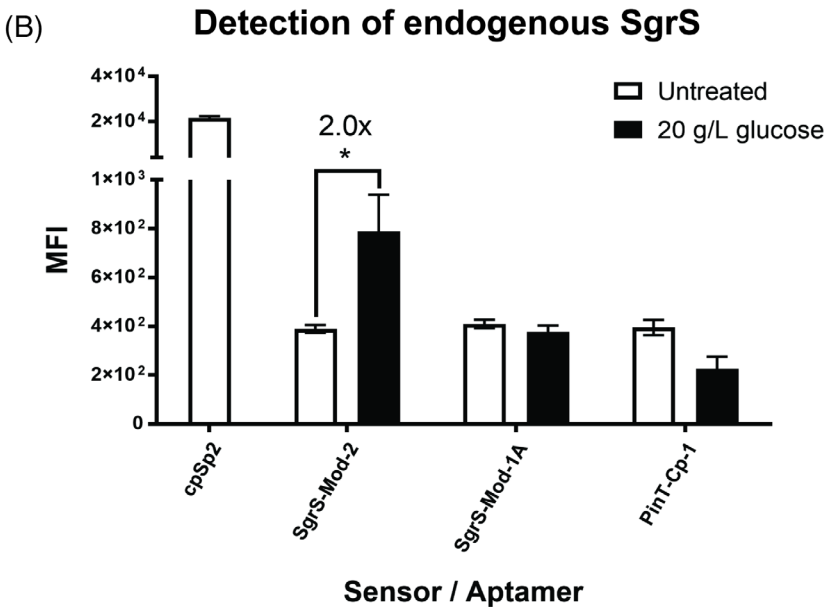


**FIGURE 5** FASTsRNA sensor response to endogenous SgrS. Flow cytometry data for FASTsRNA sensors using pRSET expression system. A, Workflow for sensor testing in *E coli*. Single plasmid expression of sensor was induced under the T7 promoter. Cells containing SgrS sensors (Srgs-Mod-2, SgrS-Mod-1A) or a control PinT sensor (PinT-Cp-1) were treated with glucose for 1.5 hours and then the MFI was measured and plotted. B, Mean fluorescence intensities for each sensor following glucose treatment for 1.5 hours

### 3.2 | FASTsRNA performance *in vivo*

Having demonstrated the *in vitro* sensing of sRNA targets, our RNA-based sensors were then analyzed for detection of these sRNA targets in *E coli*. Both sensor and target RNAs were overexpressed in *E coli* BL21 Star cells via overnight growth in autoinduction media, then the on- and off-target fluorescent response was analyzed by flow cytometry (Figure 4A). Using a pRSET-pET24a expression system, PinT-Cp-1, SgrS-Mod-2, and SgrS-Mod-1A showed statistically significant response (albeit with decreased fold activation compared to *in vitro* experiments) when expressed with their respective target RNA and no off-target response. These results demonstrate that our FASTsRNA sensors function in *E coli* and can detect overexpressed sRNAs. In contrast, PinT-Mod-1, RyhB-Cp-1, and RyhB-Mod-1A showed no fluorescent turn-on in response to their target, suggesting that some sensor designs are nontransferrable to *in vivo* applications. It should also be noted that since SgrS and RyhB are both native to *E coli*, the fluorescent signal observed for these targets may have some contribution from the endogenous sRNA target. However, in the case of overexpression, the number of copies is presumed to be significantly more than the endogenous amount, so the contribution is likely minimal in comparison.

To examine the sensor response to native sRNA levels, we chose to focus on SgrS target RNA. SgrS is known to be involved in sugar transport in *E coli* and its concentration increases upon addition of glucose. Bacterial cultures pre-transformed with pRSET sensor plasmids (SgrS sensors SgrS-Mod-2 and SgrS-Mod-1A, or PinT-Cp-1 control sensor) were grown overnight in autoinduction media to express the sensor and SgrS production was activated through addition of 20 g/L glucose, a method that has been used previously in BL21 star (DE3) *E coli*.[10] Following glucose treatment for 1.5 hours, the cells were diluted into 1X PBS buffer, DFHBI-1T was added, and the mean fluorescence intensity (MFI) was immediately measured by flow cytometry (Figure 5A). One sensor, SgrS-Mod-2, showed a 2-fold increase in fluorescence after a 1.5-hours glucose incubation period, whereas SgrS-Mod-1A showed no fluorescent response (Figure 5B). However, the PC1 control unexpectedly showed a decrease in fluorescence output in the presence of target RNA. These sensors showed significant response to an endogenous target sRNA without any modification, but previous FASTmiR designs have been improved through multiplexing strategies.[20] Therefore, it is possible that the FASTsRNA sensors described here could be further optimized through similar methods.

## 4 | CONCLUSION

In this study, we have demonstrated a computationally designed, genetically encodable RBF biosensor for the detection of bacterial sRNAs both *in vitro* and *in vivo*. The sensors with the greatest fluorescence turn-on *in vitro* were selected for *in vivo* testing. We also demonstrated that these sensors were selective for their target sequence and sensitive enough to detect changes in endogenous bacterial sRNAs. Although there were some exceptions, following the three design criteria for sensor folding in ViennaRNA yielded a > 50% success rate after screening. This method is, therefore, useful for generating candidate sequences but is not a definitive method for predicting which designs will display the desired functionality.

Although these initial screens identified sensor hits with detectable fluorescent response, sensor performance optimization is limited by the fact that they are artificially designed. Unlike natural riboswitch-based designs, one cannot access the phylogenetic sequence space to easily screen for more responsive variants. Instead, extensive engineering would be required to try to improve the sensor architecture and increase fluorescent output. Unfortunately, the otherwise reliable tRNA scaffold method for bacterial expression cannot be used for this RBF sensor due to the fact that the 5′ and 3′ ends are the sensory domains in this design.[15,41] It is possible that alternative strategies such as sensor multiplexing and alternative tRNA scaffold linkages could further improve FASTsRNA signal to allow more sensitive imaging experiments *in vivo*.

Although these RBF sensors have only been tested in *E coli* expression, we hope to transfer them to other bacterial strains to monitor sRNA levels in real-time. There is precedent for the FAST designs in mammalian cells,[20] and traditional RBF sensor designs have been employed in other bacteria. Previous work from our lab also has demonstrated that RBF sensors are sufficiently bright for quantitative flow cytometry detection (up to 35 000 individual cells are analyzed per sec) and are amenable to real-time detection by standard fluorescence microscopy, with good agreement between the results from these two methods.[16] These results demonstrate the potential of these sensors for bacterial imaging to monitor both engineered and native sRNA levels during industrial production or infection processes. With further improvement, future applications for the FASTsRNA designs may include monitoring fluctuating sRNA levels upon rapid changes in metabolism or stress response.[42,43]

### ACKNOWLEDGMENTS

This work was supported by NSF MCB-BSF grant 1815508 (to M. C. H.), NIH grant R01 GM124589 (to M. C. H.), and NIH training grant T32 GM122740 (for K. E. C.).

### CONFLICT OF INTEREST

The authors declare no conflicts of interest.

### ORCID

*Ming C. Hammond* https://orcid.org/0000-0003-2666-4764

### REFERENCES

[1] G. Storz, J. Vogel, K. M. Wassarman, *Mol. Cell* **2011**, *43*(6), 880.
[2] L. S. Waters, G. Storz, *Cell* **2009**, *136*(4), 615.
[3] M. Bobrovskyy, C. K. Vanderpool, *Front. Cell. Infect. Microbiol.* **2014**, *4* (May), 1.
[4] A. J. Westermann, K. U. Förstner, F. Amman, L. Barquist, Y. Chao, L. N. Schulte, L. Müller, R. Reinhardt, P. F. Stadler, J. Vogel, *Nature* **2016**, *529*(7587), 496.
[5] N. Nakashima, T. Tamura, L. Good, *Nucleic Acids Res.* **2006**, *34*(20), 1.

[6] D. Na, S. M. Yoo, H. Chung, H. Park, J. H. Park, S. Y. Lee, *Nat. Biotechnol.* **2013**, *31*(2), 170.
[7] J. -S. Khoo, S. -F. Chai, R. Mohamed, S. Nathan, M. Firdaus-Raih, *BMC Genomics* **2012**, *13 Suppl 7* (Suppl 7), S13, .
[8] E. Massé, S. Gottesman, *Proc. Natl. Acad. Sci. U. S. A.* **2002**, *99*(7), 4620.
[9] H. Kawamoto, Y. Koide, T. Morita, H. Aiba, *Mol. Microbiol.* **2006**, *61* (4), 1013.
[10] A. P. K. K. Karunanayake Mudiyanselage, Q. Yu, M. A. Leon-Dunque, B. Zhao, R. Wu, M. You, *J. Am. Chem. Soc.* **2018**, *140*(28), 8739.
[11] K. Ren, R. Wu, A. P. K. K. Karunanayake Mudiyanselage, Q. Yu, B. Zhao, Y. Xie, Y. Baheri, Q. Tian, M. You, *J. Am. Chem. Soc.* **2020**, *142* (6), 2968.
[12] Z. F. Hallberg, X. C. Wang, T. A. Wright, B. Nan, O. Ad, J. Yeo, M. C. Hammond, *Proc. Natl. Acad. Sci.* **2016**, *113*(7), 1790.
[13] C. A. Kellenberger, M. C. Hammond, *Methods Enzymol.* **2015**, *550*, 147.
[14] C. A. Kellenberger, S. C. Wilson, S. F. Hickey, T. L. Gonzalez, Y. Su, Z. F. Hallberg, T. F. Brewer, A. T. Iavarone, H. K. Carlson, Y.-F. Hsieh, M. C. Hammond, *Proc. Natl. Acad. Sci. U. S. A.* **2015**, *112*(17), 5383.
[15] C. A. Kellenberger, S. C. Wilson, J. Sales-Lee, M. C. Hammond, *J. Am. Chem. Soc.* **2013**, *135*(13), 4906.
[16] J. Yeo, A. B. Dippel, X. C. Wang, M. C. Hammond, *Biochemistry* **2018**, *57*(1), 108.
[17] C. A. Kellenberger, C. Chen, A. T. Whitely, D. A. Portnoy, M. C. Hammond, *J. Am. Chem. Soc.* **2015**, *137*(20), 6432.
[18] X. C. Wang, S. C. Wilson, M. C. Hammond, **2016**, *44* (17), e139.
[19] Z. F. Hallberg, Y. Su, R. Z. Kitto, M. C. Hammond, *Annu. Rev. Biochem.* **2017**, *86*, 515.
[20] K. Huang, F. Doyle, Z. E. Wurz, S. A. Tenenbaum, R. K. Hammond, J. L. Caplan, B. C. Meyers, *Nucleic Acids Res.* **2017**, *45*(14), e130.
[21] Z. M. Ying, Z. Wu, B. Tu, W. Tan, J. H. Jiang, *J. Am. Chem. Soc.* **2017**, *139*(29), 9779.
[22] W. Q. Ong, Y. R. Citron, S. Sekine, B. Huang, *ACS Chem. Biol.* **2017**, *12*, 200.
[23] Z. Wang, Y. Luo, X. Xie, X. Hu, H. Song, Y. Zhao, J. Shi, L. Wang, G. Glinsky, N. Chen, R. Lal, C. Fan, *Angew. Chem. Int. Ed.* **2018**, *57*, 972.
[24] I. L. Hofacker, *Nucleic Acids Res.* **2003**, *31*(13), 3429.
[25] S. F. Altschul, W. Gish, W. Miller, E. W. Myers, D. J. Lipman, *J. Mol. Biol.* **1990**, *215*(3), 403.
[26] A. V. Bryksin, I. Matsumura, *BioTechniques* **2010**, *48*(6), 463.
[27] W. Song, R. L. Strack, N. Svensen, S. R. Jaffrey, *J. Am. Chem. Soc.* **2014**, *136*(4), 1198.
[28] J. S. Paige, T. Nguyen-Duc, W. Song, S. R. Jaffrey, *Science* **2012**, *335* (6073), 1194.
[29] D. G. Gibson, *Methods Enzymol.* **2011**, *498*, 349.
[30] A. Ren, X. C. Wang, C. A. Kellenberger, K. R. Rajashankar, R. A. Jones, M. C. Hammond, D. J. Patel, *Cell Rep.* **2015**, *11*(1), 1.
[31] S. C. Wilson, D. T. Cohen, X. I. N. C. Wang, M. C. Hammond, *RNA* **2014**, *20*, 1153.
[32] F. W. Studier, *Protein Expr. Purif.* **2005**, *41*(1), 207.
[33] R. Strack, M. Disney, S. Jaffrey, *Nat. Methods* **2013**, *10*(12), 1219.
[34] Y. Su, S. F. Hickey, S. G. Keyser, M. C. Hammond, *J. Am. Chem. Soc.* **2016**, *138*, 7040.
[35] C. C. Brescia, P. J. Mikulecky, A. L. Feig, D. D. Sledjeski, *RNA* **2003**, *9*(1), 33.
[36] T. Moller, T. Franch, P. Hojrup, D. R. Keene, H. P. Bächinger, R. G. Brennan, P. Valentin-Hansen, *Mol. Cell* **2002**, *9*(1), 23.
[37] A. Zhang, K. M. Wassarman, J. Ortega, A. C. Steven, G. Storz, *Mol. Cell* **2002**, *9*(1), 11.
[38] B. Tjaden, S. S. Goodwin, J. A. Opdyke, M. Guillier, D. X. Fu, S. Gottesman, G. Storz, *Nucleic Acids Res.* **2006**, *34*(9), 2791.
[39] C. Monteiro, K. Papenfort, K. Hentrich, I. Ahmad, S. Le Guyon, R. Reimann, N. Grantcharova, U. Römling, *RNA Biol.* **2012**, *9*(4), 489.
[40] M. J. Wu, J. O. L. Andreasson, W. Kladwang, W. Greenleaf, R. Das, *ACS Synth. Biol.* **2019**, *8*(8), 1838.
[41] L. Ponchon, F. Dardel, *Nat. Methods* **2007**, *4*(7), 571.
[42] G. R. Richards, M. V. Patel, C. R. Lloyd, C. K. Vanderpool, *J. Bacteriol.* **2013**, *195*(21), 4816.
[43] E. Massé, C. K. Vanderpool, S. Gottesman, *J. Bacteriol.* **2005**, *187*(20), 6962.

## SUPPORTING INFORMATION

Additional supporting information may be found online in the Supporting Information section at the end of this article.

**How to cite this article:** Kitto RZ, Christiansen KE, Hammond MC. RNA-based fluorescent biosensors for live cell detection of bacterial sRNA. *Biopolymers*. 2020;e23394. https://doi.org/10.1002/bip.23394